Magnetization dynamics and the Mn^{3+} *d-d* excitation of hexagonal $HoMnO_3$ single crystals using wavelength-tunable time-resolved femtosecond spectroscopy

H. C. Shih,[1] T. H. Lin,[1] C. W. Luo,[1] J.-Y. Lin,[2] T. M. Uen,[1] J. Y. Juang,[1] K. H. Wu,[1] J. M. Lee,[3] J. M. Chen,[3] and T. Kobayashi[1,4]

[1]*Department of Electrophysics, National Chiao Tung University, Hsinchu 300, Taiwan*

[2]*Institute of Physics, National Chiao Tung University, Hsinchu 300, Taiwan*

[3]*National Synchrotron Radiation Research Center (NSRRC), Hsinchu 300, Taiwan*

[4]*Department of Applied Physics and Chemistry and Institute for Laser Science, The University of Electro-Communications, Chofugaoka 1-5-1, Chofu, Tokyo 182-8585, Japan*

(Received 20 May 2009; revised manuscript received 20 June 2009; published 30 July 2009)

We analyze the photo-induced carrier and magnetization dynamics in antiferromagnetic (AFM) $HoMnO_3$ single crystals, delineated by wavelength-dependent femtosecond spectroscopy. The emergence of long-range and short-range magnetic order are unambiguously revealed in association with an abnormal blueshift of Mn^{3+} 3*d* level around the Néel temperature and the slope variation in the temperature-dependent transient reflectivity change ($\Delta R/R$) near the Néel transition, respectively. Furthermore, the disturbance (in ps time scale) of the AFM ordering and its reordering time (in a few 100 ps time scale) are clearly identified in the negative $\Delta R/R$.

DOI: 10.1103/PhysRevB.80.024427 PACS number(s): 75.30.Et, 78.47.J−, 75.47.Lx, 75.80.+q

I. INTRODUCTION

Recently, the multiferroic manganites ($RMnO_3$) have attracted great scientific attention due to their manifestations of intriguing and significant coupling between the magnetic and electric order parameters.[1–6] The coexistence of ferroic orders in $RMnO_3$ with hexagonal (smaller ionic radius of $R=$ Sc, Y, and Ho-Lu) or orthorhombic (larger ionic radius of $R=$Eu-Dy) structure not only gives rise to rich physics of the intimate interactions between charge, orbital, lattice, and spin degrees of freedom but also some fascinating emergent physical properties which might lead to significant potential applications.[7,8] For hexagonal $HoMnO_3$ (*h*-HMO), the paraelectric (PE)-ferroelectric (FE) transition occurs at Curie temperature ($T_C \sim 875$ K) while the long-range antiferromagnetic (AFM) order appears at a much lower Néel temperature ($T_N \sim 76$ K).[9] Although it was revealed by dielectric constant and specific-heat measurements that the low-temperature magnetic phase diagram for *h*-HMO can be very complicated[10,11] due to the huge paramagnetic signal from Ho^{3+} ions, it is very difficult to unveil the AFM transition directly from the magnetization measurements. Alternatively, the second harmonic generation optical measurements or neutron scattering were used to delineate the magnetic phase transition and various spin arrangements.[12,13] It is conceived that the optical process can be a unique probe for exploring the change of magnetic properties due to its sensitivity to local magnetic ordering.[14] For instance, the interface effect between the multiferroic sample and the electrode which obscures the magnetoelectric coupling could be ruled out in optical spectroscopy, when the light probes the sample quite directly without any electrodes.[15] Recently, infrared absorption spectroscopy measurements revealed a temperature-dependent blueshift of the Mn *d* to *d* transitions (energy difference E_{dd}) in hexagonal $RMnO_3$ materials.[14,16] In particular, an unexpected extra blueshift behavior at the AFM temperature is observed. The underlying mechanism giving rise to these blueshifts, however, remains to be a matter under debate. Souchkov *et al.*[17] proposed that the blueshift might origin from the immense magnetic exchange interaction between the Mn moments, and not from effects of thermal expansion and/or magnetostriction. The magnetic ordering seems to be correlated with the main change of the electronic structure of the Mn ions in hexagonal $RMnO_3$ materials. Consequently, an appropriate method capable of simultaneously unveiling the *d-d* excitation and the associated magnetic ordering should provide some pivotal insights on these issues.

Fiebig *et al.*[18] have demonstrated that the ultrafast magnetization dynamics in AFM compounds can be probed with the second harmonic generation (SHG) by nonlinear optical techniques. This kind of characterization was not possible by the usual magneto-optical methods, such as the transmission Faraday effect and the reflective Kerr effect, due to the absence of a macroscopic magnetization. Moreover, a magnetic resonance mode exhibited in multiferroic $Ba_{0.6}Sr_{1.4}Zn_2Fe_{12}O_{22}$ has been observed by Talbayev *et al.*[19] via transient reflectance measurement. Since the magnetic order in the manganites is mainly originated from the *d* electrons residing in the e_{2g} band, it is possible that by disturbing the configuration of the *d* electrons with optical excitations some basic insights can be obtained. In this respect, owing to the different characteristic time scales for various degrees of freedom existing in these complex materials, the time-resolved spectroscopy should serve as an ideal tool to resolve the fundamental microscopic dynamics for each order parameter as well as the coupling between them. In particular, the pump-probe studies can yield such important information related to the achievable switching speeds of the multiferroic order parameters.

In this letter, we report the results of the ultrafast time-resolved evolution of magnetic effects in *h*-HMO single crystals probed by the wavelength-tunable femtosecond pump-probe technique. By manipulating the Mn^{3+} *d-d* carrier excitation with the tunable photon energy, the corresponding charge-spin coupling and magnetization dynamics

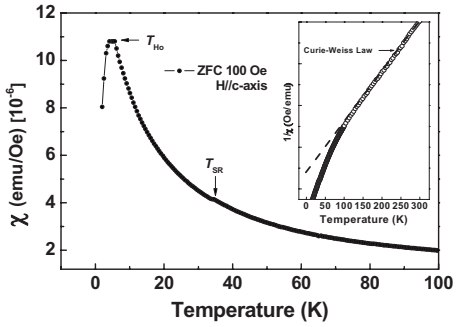

FIG. 1. The temperature-dependent susceptibility $\chi(T)$ of h-HMO with a magnetic field of 100 Oe applied along c axis. The inset shows the inverse susceptibility. The dashed line: the Curie-Weiss high-temperature extrapolation.

were subsequently identified from various parts of the transient reflectivity change curve ($\Delta R/R$, ΔR: the reflectivity change of probe pulses due to pump pulses, R: the reflectivity of probe pulses). Detailed analyses further evidence a temperature dependent blueshift in the Mn^{3+} d-d transition and an apparent effect on the energy separation of the d-electron levels resulting from the emergence of the long-range and short-range AFM ordering.

II. EXPERIMENTS

The h-HMO single crystals were grown by a traveling solvent optical floating zone method. Figure 1 shows the typical temperature-dependent magnetization $\chi(T)$ of the platelet samples. Although the expected AFM ordering of Mn moments around 76 K is hardly recognized directly from the $\chi(T)$ curve displayed in Fig. 1, a small but distinct kink occurs near 33 K. This has been previously identified as being due to the coupling between the onset of the Ho-AFM order and the Mn^{3+} moments causing the latter to rotate by an angle of 90° at T_{SR} (~33 K). The magnetic transition at $T_{Ho}\sim 5$ K, on the other hand, indicates the complete AFM order of the Ho^{3+} ions.[20] The results evidently indicate the quality and purity of the h-HMO crystal used in this study. For standard pump-probe measurements, a commercial mode-locked Ti:sapphire laser system providing short pulses (~30 fs) with repetition rate of 80 MHz and tunable wavelengths from 740 to 815 nm ($h\nu$=1.68–1.52 eV) was used. The spectral width of the output pulses was adjusted to ~25 nm (full width at half maximum) for all measurements. In order to perform the ultrafast spectroscopy, a standard pump-probe setup was employed with the fluences of 50 nJ/cm^2 and 1 nJ/cm^2 for pump beam and probe beam, respectively. The pump beam was focused on the h-HMO single crystals with the diameter of 500 μm, and the probe beam with the diameter of 300 μm was overlapped with the spot of pump beam. The polarizations of pump beam and probe beam which were perpendicular to each other were parallel to the a-b plane of h-HMO single crystals (i.e., $E\perp c$ axis). A mechanical delay stage was used to vary the time delay between pump pulses and probe pulses. The reflectivity change of a probe beam was detected by using a photodiode detector and a lock-in amplifier.

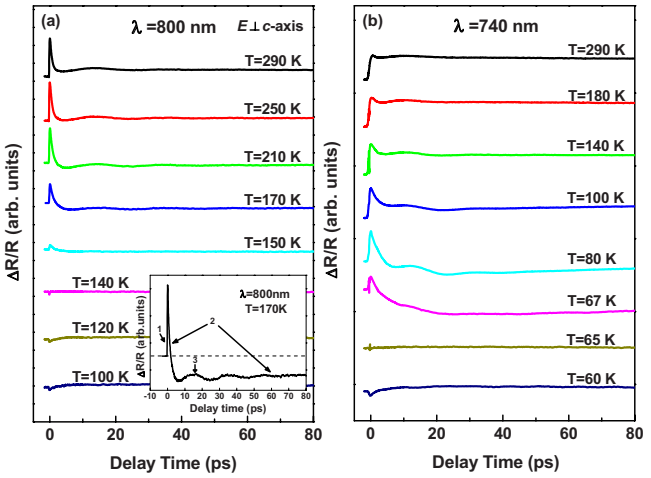

FIG. 2. (Color online) The temperature-dependent $\Delta R/R$ measured at (a) λ=800 nm and (b) λ=740 nm. The inset shows three primary features of dynamics in the $\Delta R/R$ curves.

III. RESULTS AND DISCUSSION

Figure 2 shows the typical temperature-dependent $\Delta R/R$ for the h-HMO crystals obtained at two different photon energies. Three primary features can be immediately identified in the $\Delta R/R$ curves, namely, the initial rising (excitation) component, the relaxation component, and the oscillating behavior [see the inset of Fig. 2(a), process 1–3, respectively]. For instance, for the case of λ=800 nm shown in Fig. 2(a), the amplitude of the excitation component of $\Delta R/R$ (process 1) appears to remain constant at high temperatures until it starts to drop noticeably around T=170 K. At $T\sim$150 K the amplitude of the excitation component has diminished almost completely and with $T<$140 K it even becomes negative, albeit only barely recognizable. On the contrary, the relaxation component (process 2) shows an apparent overshoot to negative $\Delta R/R$ territory which appears to grow gradually with decreasing temperature. Finally, we note that the oscillating component (process 3) behaves similarly at all temperatures and disappears altogether with the diminished excitation component. Similar results were observed for other pumping wavelengths [e.g., λ=740 nm shown in Fig. 2(b)], except for the temperature at which the amplitude of the excitation component vanishes. The oscillation in $\Delta R/R$ has been previously termed as the coherent acoustic phonon induced by the strain pulse. We note that the period of oscillation grows with the decreasing wavelength, which is consistent with those observed in hexagonal $LuMnO_3$ by Lim *et al.*[21]

In order to further explore the physical meaning of the excitation component of $\Delta R/R$ (process 1), the amplitude of $\Delta R/R$ (taken from Fig. 2. at zero delay time) as a function of temperature was measured with various pumping wavelengths (photon energies). Figure 3(a) shows that, for each photon energy used, the amplitude of $\Delta R/R$ remains essentially unchanged at higher temperature. It then drops precipitously to across zero amplitude at some characteristic temperature T_0 and becomes negative. For instance, for the case of λ=815 nm, the amplitude of $\Delta R/R$ starts to drop steeply

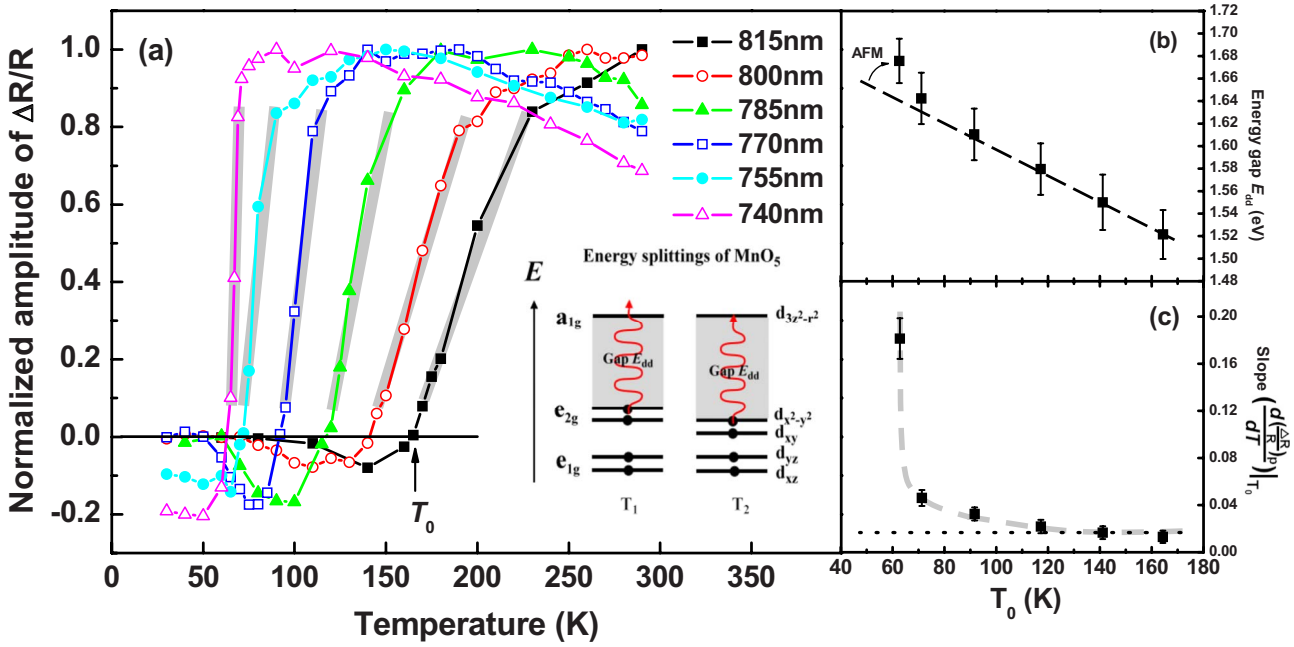

FIG. 3. (Color online) (a) The normalized amplitude of $\Delta R/R$ as a function of temperature at various wavelengths (λ) taken from Fig. 2 at zero delay time. The insets illustrate the splitting of the Mn^{3+} energy levels in the local environment MnO_5 for photon energy above and below E_{dd} ($T_1 > T_2$) (b) The energy gap E_{dd} as a function of T_0. E_{dd} is estimated from the wavelengths in (a) and the error bars are the bandwidth of laser spectrum at various center wavelengths. The dashed line is a guide to the eye emphasizing the linear behavior at high-temperature range. (c) The slope of the temperature-dependent normalized amplitude of $\Delta R/R$ in (a) (the gray thick lines) as a function of T_0 at various wavelengths. (Dashed line is a guide to the eye emphasizing the behavior of slope.)

below 220 K and across zero at $T_0 \sim 160$ K. Since the photon energy is in the range of d-d transition for the h-$R$$MnO_3$ (absorption peak $\sim$1.6 eV at room temperature),[22] the absence of the excitation component is thus a clear indication of inadequate photon energy to trigger the d-d transition [as depicted schematically in the inset of Fig. 3(a)]. The electrons residing on the e_{2g} orbital (d_{xy} and $d_{x^2-y^2}$) can transfer to the unoccupied a_{1g} orbital ($d_{3z^2-r^2}$) by absorbing pumping photons with energy exceeding E_{dd}. Conversely, this on-site Mn^{3+} E_{dd} transition will be blocked completely when the energy gap E_{dd} becomes larger than the energy of pumping photons, leading to the precipitous diminishing in the amplitude of $\Delta R/R$. The fact that T_0 gradually shifts to lower temperatures with increasing photon energy indicates that E_{dd} exhibits a blueshift with decreasing temperature [Fig. 3(b)]. This is, in fact, consistent with that observed in other h-$R$$MnO_3$ materials by Fourier transform infrared or optical spectroscopic measurements.[14,16,17]

Intuitively, the blueshift of E_{dd} might be attributed to thermal contraction of the lattice and, hence, the enhanced crystal field effect on splitting the respective d orbitals. Nevertheless, recent investigations have indicated that the blueshift of E_{dd} might be correlated with mechanisms other than simply due to the crystal-field effect associated with the symmetry distortion of the local environment of MnO_5 bipyramids.[22,23] Souchkov *et al.*,[17] based on fitting their absorption spectroscopy results and estimation of superexchange energy of h-$LuMnO_3$, argued that the unit cell volume change (only $\sim$0.3%) caused by lowering the temperature from 300 to 2 K is certainly inadequate to fully account for the relatively large change (0.2 eV or about 10% change) observed in E_{dd}. Consequently, they suggested that the blueshift in E_{dd} might be due to the emerging superexchange interaction between neighboring Mn ions, which, in turn, gives rise to a lowering of the e_{2g} levels in the AFM state while the relatively isolated a_{1g} orbital is little affected.[17] They further proposed that even the short-range AFM correlations existing in the frustrated magnetic systems like h-$R$$MnO_3$ will result in noticeable shift in the resonance energy. Within the context of this superexchange-induced effect, one expects that the blueshift in E_{dd} might turn on at temperatures much higher than the usually conceived T_N ($\sim$76 K), when the system is in the dynamical short-range ordering state. Indeed, the optical process occurs regionally and it should be sensitive to short-range magnetic order inducing the change of the electronic structure. It is interesting to note that, if we regard the photon energy as E_{dd} and plot it as a function of T_0 at which the excitation signal vanishes [as shown in Fig. 3(b)], a seemingly linear behavior [dashed line in Fig. 3(b)] is evident, indicative of a gradual increase in the extent of AFM ordering. Moreover, the behavior starts to deviate from being linear around T_N ($\sim$76 K), suggesting an extra enhancement in the blueshift of E_{dd} due to the prevailing of global long-range AFM ordering.

In order to further explore the possible connections between the magnetic ordering state and the excitation component of $\Delta R/R$ (the positive component of in $\Delta R/R$ Fig. 2), the slope of $\Delta R/R$ taken at temperatures slightly above T_0 [$d(\Delta R/R)_p/dT$ at T_0, indicated by the gray thick lines in Fig. 3(a)] as a function of the pumping photon energy is displayed in Fig. 3(c). If we attribute the blueshift of energy gap E_{dd} to being due to the short-range AFM ordering emerging

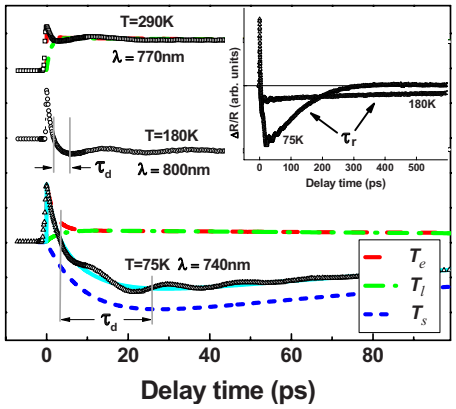

FIG. 4. (Color online) (a) The $\Delta R/R$ curves at various temperatures (T=290 K, 180 K, and 75 K). Dashed lines (red) and dash-dotted lines (green) show temperature of electrons (T_e) and lattice (T_l), respectively, due to the energy transfer by electron-lattice relaxation. The short-dashed lines (blue) show the temperature of spin system (T_s) due to spin-lattice coupling. The inset shows the reordering time (τ_r) of the disordered magnetization.

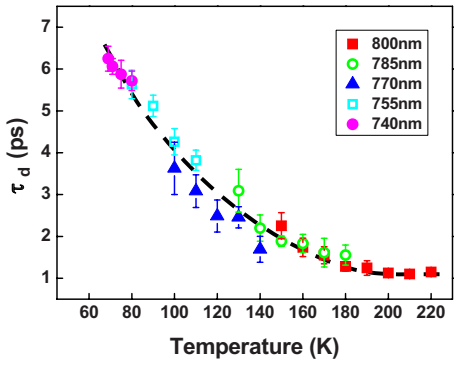

FIG. 5. (Color online) The temperature-dependent τ_d for various wavelengths. The dashed line is a guide to emphasizing the behavior of τ_d.

at temperatures far above T_N,[24] the results shown in Fig. 3(c) can thus be regarded as indications of how the AFM correlation evolves with temperature as it approaches T_N. The fact that $d(\Delta R/R)_p/dT$ increases gradually with reducing temperatures and rises sharply around T_N, thus, follows closely with the emergence of short-range to long-range-ordered AFM with decreasing temperature in this frustrated magnetic system.

Another interesting feature of the $\Delta R/R$ is the relaxation part displayed in Fig. 2 (process 2 in the inset of Fig. 2). In order to extract quantitative information and relaxation dynamics we adopted the widely used three-temperature model[25,26] to analyze the associated relaxation processes involved after excitation. In this three-temperature mode, the electrons, lattice, and spins are artificially separates by defining three independent temperatures (T_e, T_l, and T_s) that are interconnected by relaxation rates between electrons and lattice (τ_{e-l}), lattice and spins (τ_{l-s}), and electrons and spins (τ_{e-s}). After excited by laser pulses, the temperature of electron system T_e increases rapidly due to the smaller specific heat ($C_{\text{electron}} \ll C_{\text{lattice}}$).[25] Then, the electron-lattice interaction drives the system into thermal equilibrium, where electrons and lattice have the same temperature. As shown in Fig. 4, the electron-lattice thermalization within a time scale of 1 ps is depicted schematically by the dashed (red, T_e) and the dash-dotted (green, T_l) lines. In the following, the spin system interacts with lattice and reaches thermal equilibrium with characteristic time scale τ_d (the disordering time of spin system) through a spin-lattice relaxation process (schematic illustration by the short-dashed and blue line T_s in Fig. 4).[27] This raise in the temperature of spin system and the resultant disruption effects in magnetic ordering give rise to a negative $\Delta R/R$ due to the H(magnetic field)-induced redshift in the optical conductivity spectra which is opposite to the blueshift of optical conductivity spectra at lower temperatures.[16] Additionally, in materials with magnetic ordering it has been observed that the appearance of a negative component in $\Delta R/R$ due to metastable states around quasiparticle state formed by the weak electron-phonon interaction is related primarily to the disturbance of magnetic ordering.[28] After the spin-lattice thermalization, the electron, lattice, and spin systems were further cooled with characteristic time scale τ_r through a cold reservoir, e.g., sample holder. It is worth to mention that additional energy relaxation channels such as electron-electron scattering and electron-spin coupling are possible. However, for insulating AFM materials such as h-RMnO$_3$, the energy relaxation channel via the electron-spin coupling is largely blocked due to the absence of electron-electron scattering processes,[29] which would be otherwise manifested as a sub-ps component in the relaxation process.

Figure 5 shows the temperature dependence of τ_d collected from the studies with various photon energies. It is evident that τ_d increases significantly from 1 ps (at 220 K) to 6 ps (at 70 K), indicating the prominent role played by the state of magnetic ordering. Furthermore, the monotonic and seemingly universal behavior again indicates that it needs longer time to disturb the spin system when the magnetic ordering is more robust at lower temperatures due to the prevailing of the long-range AFM ordering. The magnetic ordering disturbed by spin-lattice coupling (increase T_s) has to be somehow reordered, i.e., the cooling of spin system. In this case, one expects that, due to the competition between the AFM superexchange interaction and thermal energy, the disturbed magnetic ordering should spend shorter time to reorder at lower temperatures. Indeed, as shown in the inset of Fig. 4, we can identify that the characteristic reordering time τ_r is about 120 and 610 ps for T=75 K and T =180 K, respectively. Ju *et al.*[30] revealed the dynamics of the AFM ordering in the NiO layer by measuring the magnetization rotation in the NiFe/NiO multilayer system. They reported that the reordering time of demagnetization in AFM is on the time scale of 100 ps which is consistent with that obtained in the current pump-probe measurements.

IV. SUMMARY

In summary, the ultrafast dynamics associated with the Mn^{3+} d-d excitation in h-HMO single crystals were studied by measuring $\Delta R/R$ using the femtosecond spectroscopy.

The results clearly display several characteristic excitation and relaxation components with their own distinctive temperature and photon-energy dependences. The amplitude of the initial rising component of $\Delta R/R$ corresponding to the Mn^{3+} *d-d* excitation is caused by strong coupling between the electronic structure and AFM ordering. By combining with the analyses on the subsequent relaxation processes associated with magnetization dynamics, the detected blueshift is believed to originate primarily from the emergence of the AFM superexchange interaction between the neighboring Mn^{3+} ions.

ACKNOWLEDGMENTS

This work was supported by National Science Council (Grants No. NSC 95-2112-M-009-037-MY3 and NSC 95-2112-M-009-011-MY3) and the MOE-ATU program at NCTU.

[1] T. Lottermoser, T. Lonkai, U. Amann, D. Hohlwein, J. Ihringer, and M. Fiebig, Nature (London) **430**, 541 (2004).
[2] S.-W. Cheong and M. Mostovoy, Nat. Mater. **6**, 13 (2007).
[3] T. Kimura, T. Goto, H. Shintani, K. Ishizaka, T. Arima, and Y. Tokura, Nature (London) **426**, 55 (2003).
[4] N. A. Spaldin and M. Fiebig, Science **309**, 391 (2005).
[5] T. H. Lin, H. C. Shih, C. C. Hsieh, C. W. Luo, J.-Y. Lin, J. L. Her, H. D. Yang, C.-H. Hsu, K. H. Wu, T. M. Uen, and J. Y. Juang, J. Phys.: Condens. Matter **21**, 026013 (2009).
[6] R. Schmidt, W. Eerenstein, and P. A. Midgley, Phys. Rev. B **79**, 214107 (2009).
[7] C. W. Nan, M. I. Bichurin, S. Dong, D. Viehland, and G. Srinivasan, J. Appl. Phys. **103**, 031101 (2008).
[8] N. Hur, S. Park, P. A. Sharma, J. S. Ahn, S. Guha, and S.-W. Cheong, Nature (London) **429**, 392 (2004).
[9] F. Yen, C. R. dela Cruz, B. Lorenz, Y. Y. Sun, Y. Q. Wang, M. M. Gospodinov, and C. W. Chu, Phys. Rev. B **71**, 180407(R) (2005).
[10] B. Lorenz, A. P. Litvinchuk, M. M. Gospodinov, and C. W. Chu, Phys. Rev. Lett. **92**, 087204 (2004).
[11] F. Yen, C. dela Cruz, B. Lorenz, E. Galstyan, Y. Y. Sun, M. Gospodinov, and C. W. Chu, J. Mater. Res. **22**, 2163 (2007).
[12] M. Fiebig, C. Degenhardt, and R. V. Pisarev, J. Appl. Phys. **91**, 8867 (2002).
[13] A. Muñoz, J. A. Alonso, M. J. Martínez-Lope, M. T. Casáis, J. L. Martínez, and M. T. Fernández-Díaz, Chem. Mater. **13**, 1497 (2001).
[14] W. S. Choi, S. J. Moon, Sung Seok A. Seo, D. Lee, J. H. Lee, P. Murugavel, T. W. Noh, and Y. S. Lee, Phys. Rev. B **78**, 054440 (2008).
[15] R. Schmidt, W. Eerenstein, T. Winiecki, F. D. Morrison, and P. A. Midgley, Phys. Rev. B **75**, 245111 (2007).
[16] R. C. Rai, J. Cao, J. L. Musfeldt, S. B. Kim, S.-W. Cheong, and X. Wei, Phys. Rev. B **75**, 184414 (2007).
[17] A. B. Souchkov, J. R. Simpson, M. Quijada, H. Ishibashi, N. Hur, J. S. Ahn, S. W. Cheong, A. J. Millis, and H. D. Drew, Phys. Rev. Lett. **91**, 027203 (2003).
[18] M. Fiebig, N. P. Duong, T. Satoh, B. B. V. Aken, Ke. Miyano, Y. Tomioka, and Y. Tokura, J. Phys. D **41**, 164005 (2008).
[19] D. Talbayev, S. A. Trugman, A. V. Balatsky, T. Kimura, A. J. Taylor, and R. D. Averitt, Phys. Rev. Lett. **101**, 097603 (2008).
[20] B. Lorenz, F. Yen, M. M. Gospodinov, and C. W. Chu, Phys. Rev. B **71**, 014438 (2005).
[21] D. Lim, R. D. Averitt, J. Demsar, A. J. Taylor, N. Hur, and S. W. Cheong, Appl. Phys. Lett. **83**, 4800 (2003).
[22] W. S. Choi, D. G. Kim, Sung Seok A. Seo, S. J. Moon, D. Lee, J. H. Lee, H. S. Lee, D.-Y. Cho, Y. S. Lee, P. Murugavel, J. Yu, and T. W. Noh, Phys. Rev. B **77**, 045137 (2008).
[23] D.-Y. Cho, S.-J. Oh, D. G. Kim, A. Tanaka, and J.-H. Park, Phys. Rev. B **79**, 035116 (2009).
[24] Th. Lonkai, D. G. Tomuta, and J.-U. Hoffmann, J. Appl. Phys. **93**, 8191 (2003).
[25] R. D. Averitt and A. J. Taylor, J. Phys.: Condens. Matter **14**, R1357 (2002).
[26] G. M. Müller, J. Walowski, M. Djordjevic, G.-X. Miao, A. Gupta, A. V. Ramos, K. Gehrke, V. Moshnyaga, K. Samwer, J. Schmalhorst, A. Thomas, A. Hütten, G. Reiss, J. S. Moodera, and M. Münzenberg, Nat. Mater. **8**, 56 (2009).
[27] A. V. Kimel, A. Kirilyuk, A. Tsvetkov, R. V. Pisarev, and Th. Rasing, Nature (London) **429**, 850 (2004).
[28] Y. H. Ren, M. Ebrahim, H. B. Zhao, G. Lüpke, Z. A. Xu, V. Adyam, and Qi Li, Phys. Rev. B **78**, 014408 (2008).
[29] T. Ogasawara, K. Ohgushi, Y. Tomioka, K. S. Takahashi, H. Okamoto, M. Kawasaki, and Y. Tokura, Phys. Rev. Lett. **94**, 087202 (2005).
[30] G. Ju, A. V. Nurmikko, R. F. C. Farrow, R. F. Marks, M. J. Carey, and B. A. Gurney, Phys. Rev. Lett. **82**, 3705 (1999).